

GPPS-TC-2022-136

Development of a surrogate model for uncertainty quantification of compressor performance due to manufacturing tolerance

Quentin Rendu
Imperial College London
quentin.rendu@gmail.com
London, UK

Loic Salles
Imperial College London
London, UK

ABSTRACT

In gas turbine and jet engines, stagger angle and tip gap variations between adjacent blades lead to the deterioration of performance. To evaluate the effect of manufacturing tolerances on performances, a CFD-based uncertainty quantification analysis is performed in this work. However, evaluating dozens of thousands of rotor assembly through CFD simulations would be computationally prohibitive. A surrogate model is thus developed to predict compressor performance given an ordered set of manufactured blades. The model is used to predict the influence of tip gap and stagger angle variations on maximum isentropic efficiency. The results confirm that the best arrangement is obtained by minimizing the stagger angle variation between adjacent blades, and by maximizing the tip gap variation. Another finding is that the best arrangement yields the lowest variability, the range of maximum efficiency being 4 times sharper (resp. 2 times) than worst arrangement for stagger angle variations (resp. tip gap variations). Not measuring manufacturing tolerances, or not specifying any strategy for the blade arrangement, lead to variability as large as the worst arrangement.

INTRODUCTION

Aerodynamic design of gas turbines and jet engines relies on the assumption of infinitely accurate geometry and boundary conditions. Analytical models and CFD simulations are performed using these ideal conditions as input, as well as circumferential periodicity which assumes that all the blades are identical. However, the manufactured engine will always exhibit geometry variability due to the manufacturing process. The impact of this variability on the performances is of prior importance.

The variability of a compressor performance due to uncertain inlet total pressure profile has been tackled using probabilistic CFD (Gopinathrao et al., 2009) and Monte-Carlo simulation (Loeven and Bijl, 2010). Lavainne (Lavainne, 2003) used both deterministic and probabilistic simulations to investigate the effect of manufacturing tolerances on the performances of a compressor stage. He found out that variability in tip clearance has the strongest effect (when compared to chord, maximum thickness, leading edge and trailing edge thickness). More recently, the influence of geometric tolerances on performances have been studied both for turbine (Montomoli et al., 2011; Kolmakova et al., 2014) and for compressors (Lange et al., 2012; Liu et al., 2014; Ma et al., 2019). These works rely either on measurements of the blade geometry (Lange et al., 2012; Kolmakova et al., 2014; Ma et al., 2019) or on parametric study (Montomoli et al., 2011; Liu et al., 2014).

The behavior of a transonic compressor is mostly affected by variations of stagger angle (the angle between the blade's chord and the rotational axis) and tip gap (the clearance between blade's tip and the casing). The former influences the loading of each blade and the shock-wave position, which shifts the characteristic curve and affect the efficiency, while the latter is responsible for losses and secondary flows which can trigger rotating instabilities. An illustration of the effect of stagger angle and tip gap variations on NASA rotor 67 performances is shown in Fig. 1.

Once assembled in a rotor assembly, blades with geometry variability lead to a degradation of performances. This is due to the average effect of geometrical tolerances and to the variation between adjacent blades. In other words, the order in which the blades are arranged influences the performances, as shown in previous work (Suriyanarayanan et al., 2022).

In the first design steps, the main concern is not the optimal arrangement but the uncertainty quantification of the compressor performance. Full-annulus numerical simulations can be used in industry to assess the behavior of a specific arrangement but are computationally prohibitive to evaluate thousands of them. To overcome this, a surrogate model has

been developed in this work. It relies on physical insights and meta-modelling to greatly reduce the computational costs. Most of the physical phenomena are captured thanks to inexpensive single-passage and double-passage computations. The model, which can quickly output a performance curve for a given set of blade, can then be used for the uncertainty quantification study.

In the first part of the paper, the flow solver, the test cases and the different blade arrangements are presented. The surrogate model for stagger angle and tip gap variation is then described and validated against CFD data. Finally, the model is used to perform an uncertainty quantification of compressor performance due to manufacturing tolerances.

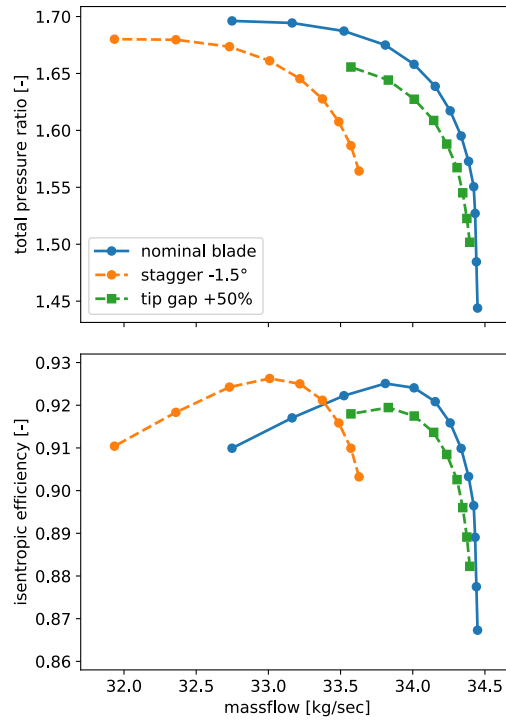


Figure 1 EFFECT OF STAGGER ANGLE AND TIP GAP VARIATION ON NASA ROTOR 67 TOTAL PRESSURE RATIO AND ISENTROPIC EFFICIENCY

1 METHODOLOGY

In this section the numerical models, the test cases and the blade arrangements are presented.

1.1 Flow Solver

The simulations were performed using the in-house CFD solver AU3D, developed at Imperial College London-VUTC over last 30 years. AU3D is a three dimensional, time-accurate, viscous, compressible Reynolds Averaged Navier-Stokes (RANS) solver that uses Spalart-Allmaras (SA) model to evaluate the turbulent eddy viscosity. The solver operates on a semi-structured mesh with hexahedral elements found around the airfoil and prismatic elements in rest of the passage. The boundary layer region in rotor-to-rotor grid has a body-fitted O grid while rest of the region is unstructured. The tip clearance geometry is meshed by triangulating the blade tip and mapping extra layers over the tip (Sayma et al., 2000). The flow solver is based on vertex-centered finite volume method. Inviscid fluxes are discretised by JST central scheme with matrix artificial dissipation and a pressure switch in the vicinity of discontinuities. The resulting system of equations is advanced in time using an implicit scheme with Jacobi iteration and dual time stepping. The solver has been successful in predicting the design and off-design conditions of turbomachinery (Dodds and Vahdati, 2015; Vahdati and Imregun, 1996; Lee et al., 2018).

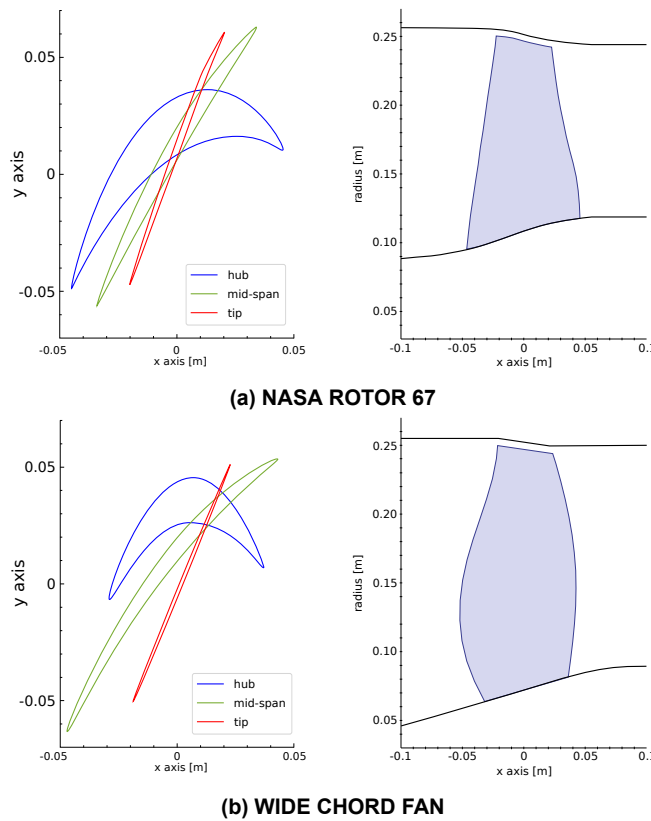
1.2 Test Cases

Two different fans are considered in this study. The first one is NASA Rotor 67 (Strazisar et al., 1989), a highly tip loaded fan for which lots of experimental and numerical data is available. The second one is a wide chord fan representative of modern engines. The characteristic features of the two test cases are shown in Table 1.

Table 1 COMPARISON OF TEST CASES (DESIGN POINT)

	NASA rotor 67	Wide chord fan
Number of blades	22	18
Rotational speed	16043 rpm	12650 rpm
Pressure ratio	1.63	1.26
Massflow	33.3 kg/sec	36.7 kg/sec
Tip gap	0.6mm	0.9mm

To visualize the differences between the two test cases, a meridional view and the airfoils at hub, mid-span and tip sections are plotted in Fig. 2a for NASA rotor 67 and in Fig. 2b for the wide chord fan. The hub to tip ratio is smaller for the wide chord fan, which is typical of high by-pass ratio fan which rely on large massflow and low rotational speed to produce thrust. The radial profile of total pressure ratio (normalized by its value at design point) is shown for both test cases in Fig. 3. The maximum pressure ratio is obtained at the tip for NASA rotor 67 and around 40% span for the wide chord fan.

**Figure 2 AIRFOILS AND RADIAL VIEW OF TEST CASES**

A mesh size of 1 million points per passage was used for both the test cases based on a mesh convergence study. Single, double passage, and full annulus computations will be used. For all these cases, total pressure, total temperature and flow angles are specified at the inlet boundary. Downstream of the rotor, there is a convergent nozzle and the outlet where low back-pressure is imposed. Thus, the nozzle is choked and ensures that disturbances from the exit do not propagate upstream (Vahdati et al., 2005). To generate the characteristic curve at a given speedline, from choke to stall point, the downstream nozzle is gradually closed, reducing the massflow.

To represent stagger angle manufacturing tolerances, a twist is imposed to the blade by using mesh morphing. Following previous work (Suriyanarayanan et al., 2022), the variation of stagger angle is in the range of $\pm 1.5^\circ$. The tip gap variations do not impact the performances of the wide chord fan which is not tip-loaded (see Fig. 3). Therefore, only NASA rotor 67 will be considered. Five meshes have been generated with five different gaps, ranging from 0.3mm to 1.5mm (50% to 250% of nominal tip gap).

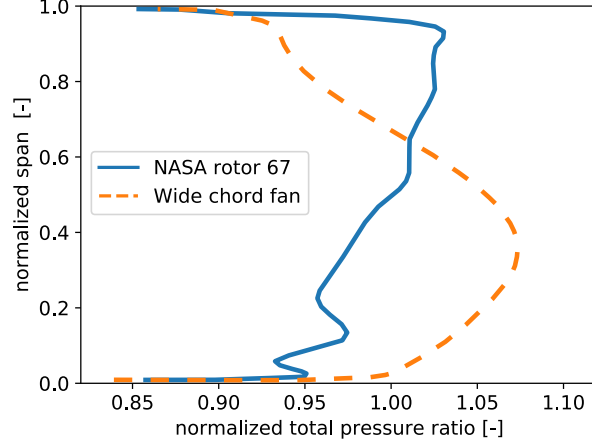


Figure 3 RADIAL PROFILE OF TOTAL PRESSURE RATIO FOR THE TWO TEST CASES

1.3 Blade Arrangement

Blades with manufacturing tolerances are, by definition, no longer identical. As a consequence, given a set of manufactured blades, the arrangement may have an impact on compressor performance. For any geometric feature ϕ , two extreme cases can be considered:

- minimizing the variation of ϕ between adjacent blades, resulting in a smooth pattern shown in Fig. 4b for stagger angle
- maximizing the variation of ϕ between adjacent blades, resulting in an alternated pattern shown in Fig. 4c for stagger angle

To be consistent with previous published work, the smooth pattern will be referred as "sinusoidal" while the alternated one will be referred as "zigzag".

Given a set of N blades with different values for ϕ , finding the arrangements yielding sinusoidal and zigzag patterns is a problem in combinatorial optimization. One can reframe the problem by computing the difference $\Delta\phi$ between each blade and all the others. This quantity can be seen as a distance and the problem becomes equivalent to the travelling salesman problem (finding the shortest path crossing a given set of cities, the distance between them being known). In this work, the equivalent travelling salesman problem was solved using a genetic algorithm (Kirk, 2014).

2 SURROGATE MODEL

The goal of the surrogate model is to output the characteristic curve of a compressor at a given speed knowing the blade distribution. An example is shown in Fig. 5 for a 6 blades rotor with three different blade geometry (tip gap or stagger variation). First, one has to choose a blade arrangement. Without loss of generality, a symmetric pattern has been used to simplify the example. Once the input (i.e. an ordered blade distribution) is defined, the model sweeps through each pair of adjacent blades and computes the characteristic curve of an equivalent compressor, consisting of these two blades arranged in an alternated pattern. An exact solution can be achieved by using double passage simulations with periodic boundary conditions, or by using meta-modelling from a sample of CFD solutions. To obtain the performances of the targeted blade arrangement, the equivalent compressors characteristic curves are mass-averaged. Formally, the massflow \dot{m} , the total pressure ratio PR and the isentropic efficiency η are given by

$$\dot{m} = \frac{\sum_i^N \dot{m}_i}{N} ; \quad \text{PR} = \frac{\sum_i^N \dot{m}_i \text{PR}_i}{\sum_i^N \dot{m}_i} ; \quad \eta = \frac{\sum_i^N \dot{m}_i \eta_i}{\sum_i^N \dot{m}_i} \quad (1)$$

where N is the number of blades, \dot{m}_i the massflow, PR_i the total pressure ratio and η_i the isentropic efficiency of the equivalent compressor consisting of blades i and $i + 1$.

This strategy allows the model to compute the effect of the blade i on itself and its neighbors ($i - 1$ and $i + 1$). The influence on blades further apart ($i + 2$ and $i - 2$) is assumed to be of lower order, which is confirmed by the results presented in section 2.1.

Previous work (Suriyanarayanan et al., 2022) has shown that tip gap variations affect both stall margin and performance whereas stagger angle variations mostly affect the latter. While relying on the same strategy, two independent surrogate models are needed to compute the characteristic curve of equivalent compressors (see the middle-part of Fig. 5).

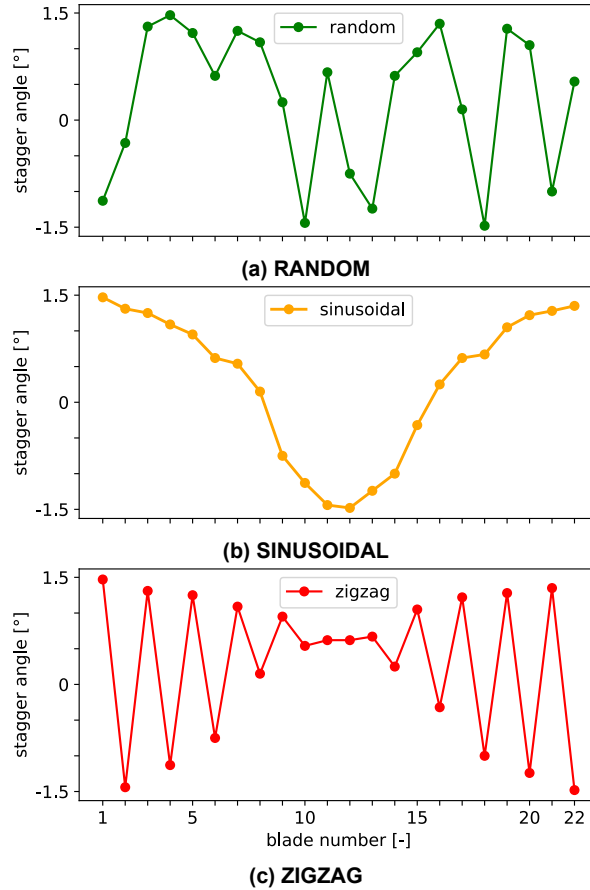


Figure 4 DIFFERENT ARRANGEMENTS FOR A GIVEN SET OF 22 BLADES WITH STAGGER ANGLE VARIATION

2.1 Stagger Angle Variations

Concerning stagger angle, the surrogate model must take into account two effects. The first one is a shift in average stagger angle. If the input is a set of identical blades at a stagger angle different than the designed geometry, the incidence would change and the characteristic curve would shift. This effect can be accurately modelled by single-passage computations with different stagger angle. Characteristic curves are computed for different stagger angle and linear interpolation is used to recover any value of average stagger angle. Fig. 6a shows how to recover an angle of 0.34° for instance.

Once the average stagger angle is correctly modelled, one needs to introduce the effect of stagger variation between two adjacent blades, which we will call adjacent mis-stagger. This effect can be estimated by running double passage computations, which represent a rotor with two sets of blades arranged in an alternated pattern. Keeping the average stagger angle constant (for instance 0° , which corresponds to the designed geometry), one can isolate the effect of adjacent mis-stagger. Using double passage computations, it is possible to reconstruct the effect of any adjacent mis-stagger by interpolation, as shown in Fig. 6b with 0.92° for instance.

A convergence study has been done to evaluate the number of points needed to achieve a satisfactory interpolation. The comparison of predicted total pressure ratio with full annulus computations is shown in Fig. 7a for Rotor 67 and in Fig. 7b for the wide chord fan. 5 single passage computations (-1.5° , -1° , 0° , 1° , 1.5°) and two double passage computations ($\pm 1^\circ$ and $\pm 1.5^\circ$) were chosen, yielding a maximum error on total pressure ratio of 0.2%.

2.2 Tip Gap Variations

Tip gap variations quickly lead to non-linear effects on stall margin and performance. In that case, simple linear interpolation did not prove sufficient to build a reliable surrogate model. To overcome this issue, free parameters have been added in the averaging process. The resulting formula, which is referred as smart average, is given by

$$\text{PR} = \frac{\sum_i^N \alpha \dot{m}_i^\beta \text{PR}_i^\kappa}{\sum_i^N \dot{m}_i^\delta} \quad (2)$$

Using full-annulus computations as target values, the parameters are computed using a non linear least square optimization. Concerning the performance prediction, it is more effective to work with a scaled total temperature ratio rather

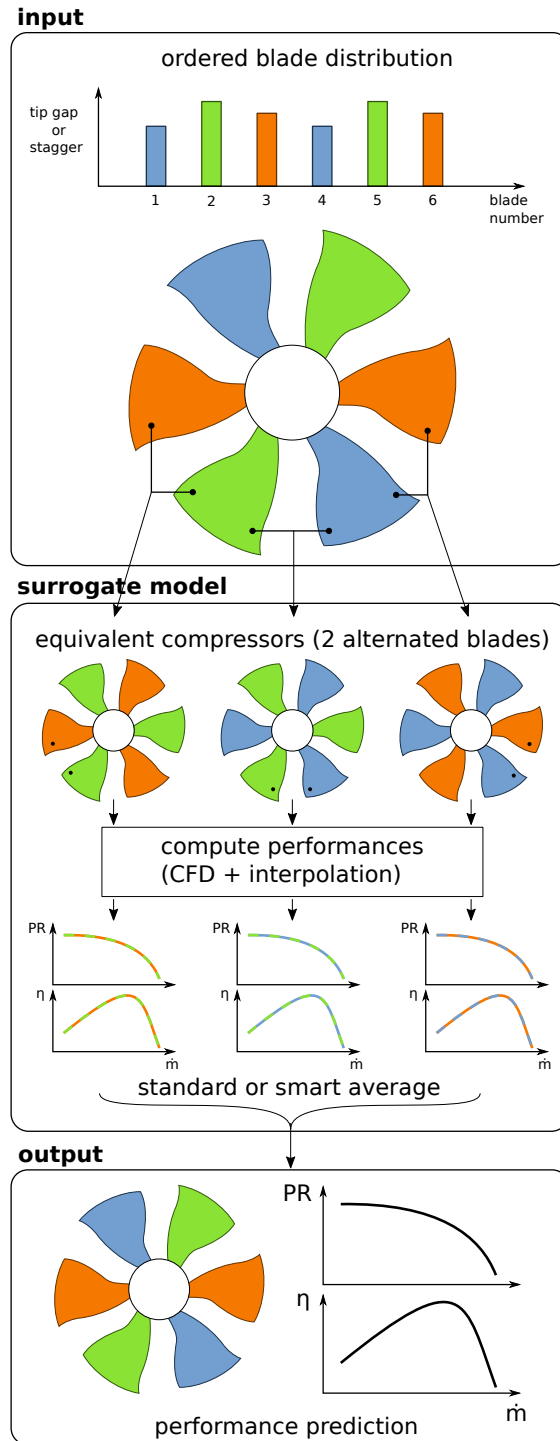
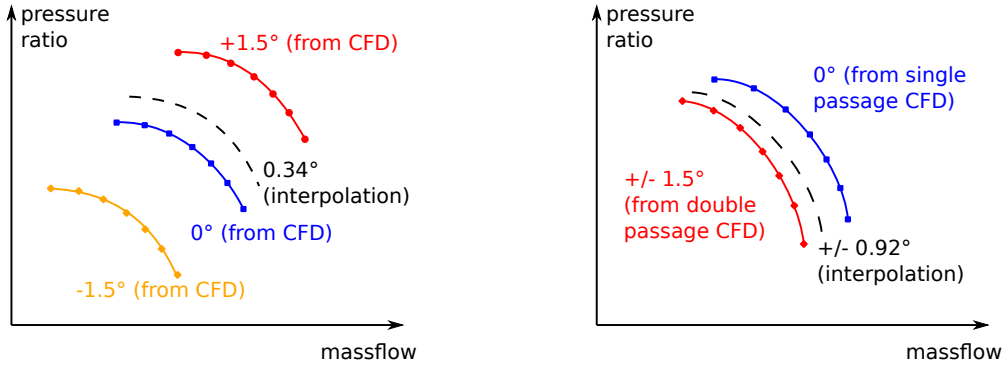


Figure 5 FRAMEWORK FOR THE SURROGATE MODEL

than with isentropic efficiency. Indeed, total pressure ratio curve is monotonic while isentropic efficiency curve exhibits a maximum at design point. The two curves cannot be superimposed, a different set of parameters would thus be needed for each of them, increasing the need of training data. On the other hand, we know that for isentropic transformation,

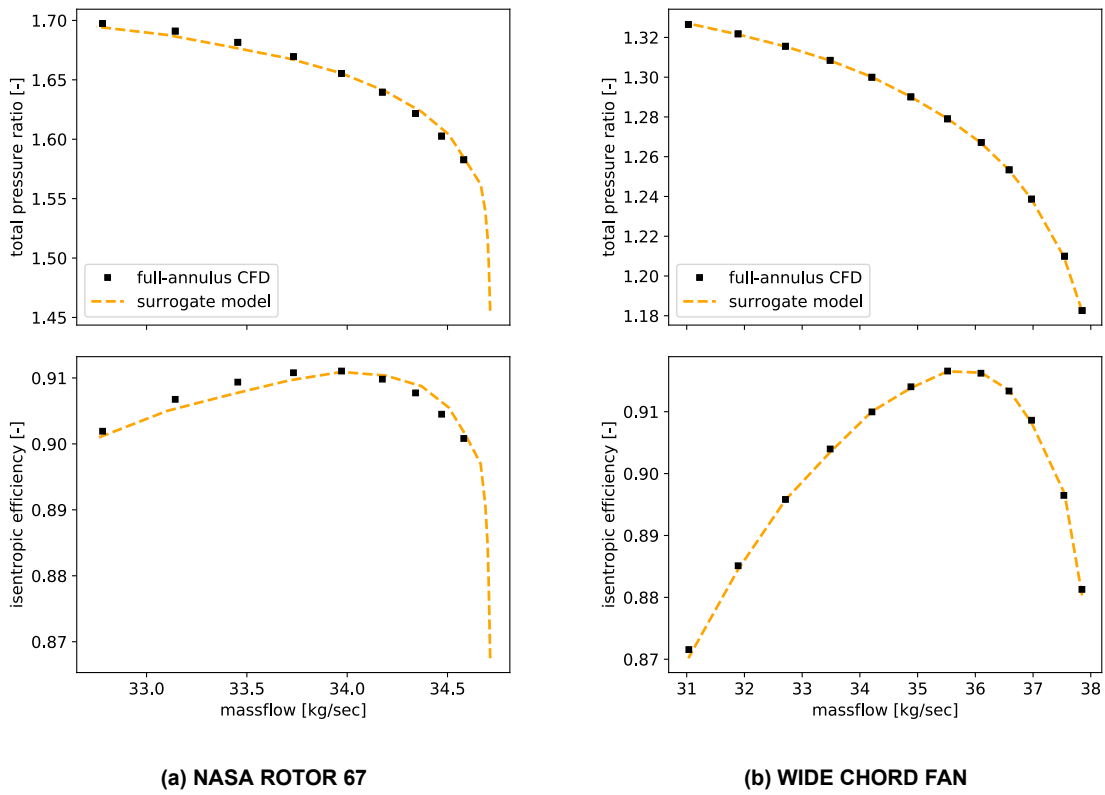
$$PR = TR^{\frac{\gamma}{\gamma-1}} \quad (3)$$

The curve of total temperature ratio raised to the power $\frac{\gamma}{\gamma-1}$ is similar to the curve of total pressure ratio, hence the same set of parameters is used. This step can be seen as a physics-informed normalization of the data prior to the training



(a) AVERAGE STAGGER ANGLE (SINGLE PASSAGE CFD) (b) ADJACENT MIS-STAGGER (DOUBLE PASSAGE CFD)

Figure 6 INTERPOLATION STRATEGY FOR STAGGER ANGLE VARIATIONS



(a) NASA ROTOR 67

(b) WIDE CHORD FAN

Figure 7 COMPARISON OF SURROGATE MODEL PREDICTIONS FOR STAGGER VARIATION WITH CFD FULL-ANNULUS RESULTS

phase. The smart average formula for the total temperature ratio is

$$TR = \frac{\sum_i^N \alpha m_i^\beta TR_i^\kappa}{\sum_i^N m_i^\delta} \quad (4)$$

A comparison of standard and smart average with full-annulus CFD is given in Fig. 8. The maximum relative error on total pressure ratio is 2.6% for the standard average and 1.3% for the smart average. The extra-cost of this improved prediction is 5 full-annulus computations to calibrate the model parameters. In this work, the parameters have been computed for a given rotational speed and a specific blade geometry. If the discrepancies between full-annulus and standard average are expected to show a general trend (always under-predicting performances for instance), a unique set of parameter can be sought for different speed and geometries to reduce the cost of the surrogate model while improving prediction with respect to standard average. Such a study is beyond the scope of the paper.

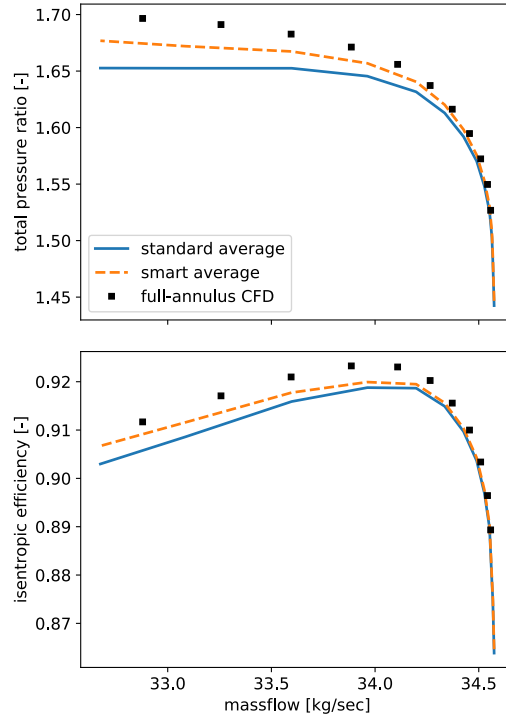


Figure 8 COMPARISON OF STANDARD AND SMART AVERAGE SURROGATE MODEL WITH FULL-ANNULUS CFD FOR ROTOR 67

This section presented the strategy of the surrogate model used in this paper for stagger angle and tip gap variations, as well as its validation against CFD data. In the next section, the surrogate model will be used to investigate the impact of manufacturing tolerances on performances.

3 UNCERTAINTY QUANTIFICATION

Uncertainty quantification can be used to assess the variability of a design with respect to manufacturing tolerances. Using manufactured blades, one can compute the range of these tolerances and their distribution (gaussian, uniform, ...). In this work, we consider uniform continuous distributions of stagger variations between -1.5 and $+1.5$ and uniform discrete tip gap variations (5 equally spaced values between 0.2% span and 1% span).

To ensure that all the design space is spanned, 50,000 thousands sets of blade are generated. Each set of blades can then be assembled in any order, resulting in one rotor configuration (we assume that the structural dynamic balancing is done afterwards and do not constrain the choice of blade arrangement).

Previous work (Suriyanarayanan et al., 2022) showed that stagger angle variations create a change in passage geometry and incidence angle which induce a displacement of the shock-wave. The maximal efficiency is obtained, by design, for a specific shock-wave position which is, by symmetry, the same for all passages. Mis-stagger between adjacent blades breaks the annular symmetry and creates a displacement of the shock-waves, leading to a less efficient configuration. Hence, to maximize compressor performance, one needs to minimize adjacent mis-stagger (which is referred as sinusoidal pattern).

For a set of blades with identical tip clearance at peak efficiency, each blade generates its own leakage flow. When getting closer to stall, the leakage flow of adjacent blades can merge and create rotating stall cells, breaking the annular symmetry (or at least reducing the wave-number of the periodic pattern). To maximize the compressor performance, one needs to contain the leakage flow of each blade. Given a blade with a large tip clearance, placing a blade with small tip clearance right after it will stop the leakage flow. Hence, to maximize compressor performance, one needs to maximize adjacent tip-gap variations (which is referred as zigzag pattern). More details on these two mechanisms can be found in (Suriyanarayanan et al., 2022).

The surrogate model allows us to arrange each set of blades along any pattern and to plot the resulting performances envelope. This work focuses on three arrangements: sinusoidal, zigzag and random (which can be considered as baseline).

3.1 Stagger Angle Variations

The effect of stagger variations on maximum isentropic efficiency is plotted in Fig. 9a for Rotor 67 and in Fig. 9b for the wide chord fan. As expected, the worst performances are given by zigzag arrangement while the best ones are obtained using the sinusoidal pattern. More interestingly, the range of efficiency depends on the chosen arrangement.

For rotor 67 and the wide chord fan, arranging the blades in a sinusoidal pattern guarantees that narrowest envelope, whereas it is widest for the zigzag pattern. This is more evident when looking at the probability density function against average stagger angle, plotted in Fig. 10 for rotor 67. It shows that the maximum isentropic efficiency fits in the range [92%-92.5%] for sinusoidal arrangement, which is four times narrower than the range [90.5%-92.2%] obtained for the zigzag arrangement. Same conclusions can be drawn from the wide chord fan results, indicating that the results are geometry independent.

While these two configurations are representative of the best and the worst case, random arrangement has also been evaluated. It is representative of a process where no arrangement strategy is chosen or where information on manufactured blade geometry is not available. The width of the envelope for random arrangement is similar to the zigzag arrangement envelope, indicating large variability.

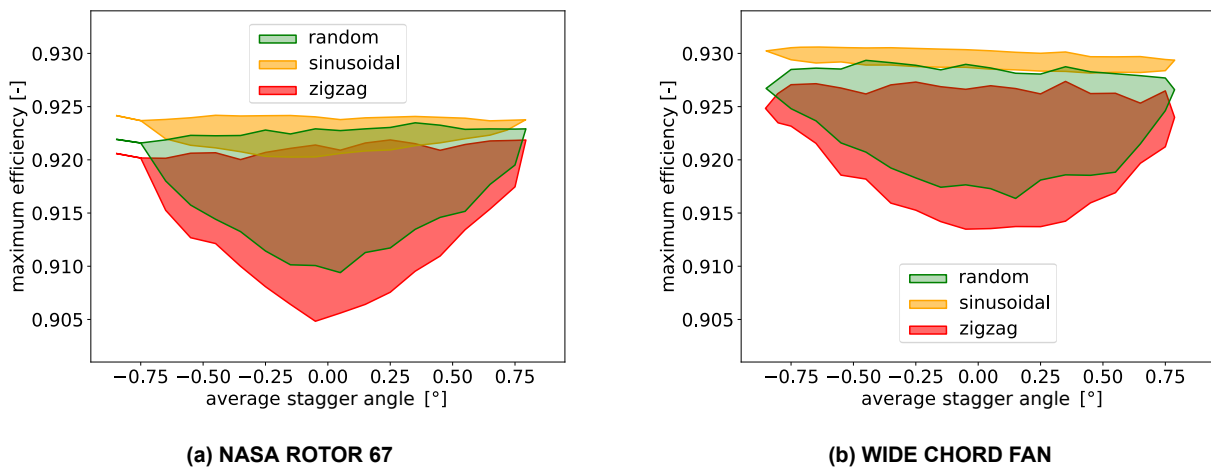


Figure 9 ENVELOPE OF MAXIMUM ISENTROPIC EFFICIENCY AGAINST AVERAGE STAGGER ANGLE FOR THREE DIFFERENT ARRANGEMENTS

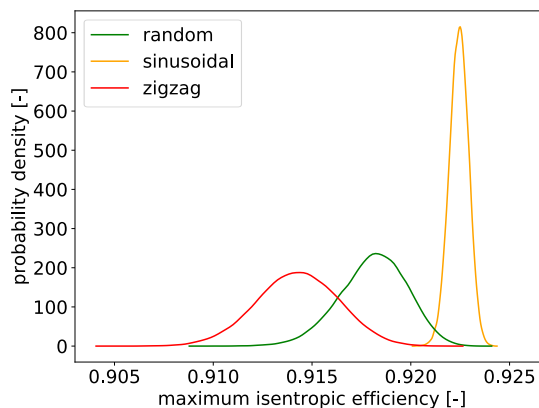


Figure 10 PROBABILITY DENSITY AGAINST MAXIMUM ISENTROPIC EFFICIENCY FOR DIFFERENT BLADE ARRANGEMENTS ON ROTOR 67

3.2 Tip Gap Variations

By its design which maximize the loading at mid span, the wide chord fan is insensitive to tip gap variations. Hence, only rotor 67 will be used in this section to evaluate the effect of tip gap variations on performances.

The effect on maximum isentropic efficiency is plotted in Fig. 11. As expected, a general trend with negative slope is observed, reflecting the increase in losses when the tip clearance opens. The best and worst performances are associated with

zigzag and sinusoidal pattern respectively, which confirm previous work. Similarly to the UQ study on stagger variations, the envelope width is small for the best arrangement and large for the worst one. Random arrangement gives in-between performances but variability as large as the worst arrangement.

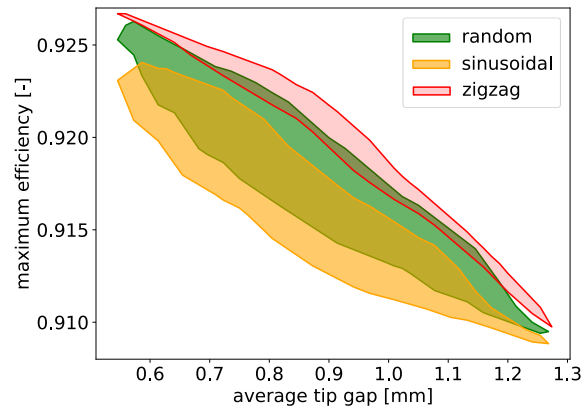


Figure 11 ENVELOPE OF MAXIMUM ISENTROPIC EFFICIENCY AGAINST AVERAGE TIP GAP FOR DIFFERENT BLADE ARRANGEMENTS

To further investigate and to quantify the variability of efficiency with respect to different arrangement, the vertical width of the maximum efficiency envelope is plotted against average tip gap in Fig. 12. For an average tip gap equal to 0.9mm, the envelope is twice as wide for sinusoidal and random arrangement, when compared to zigzag, indicating once again that the best arrangement on performances is associated with the lowest variability.

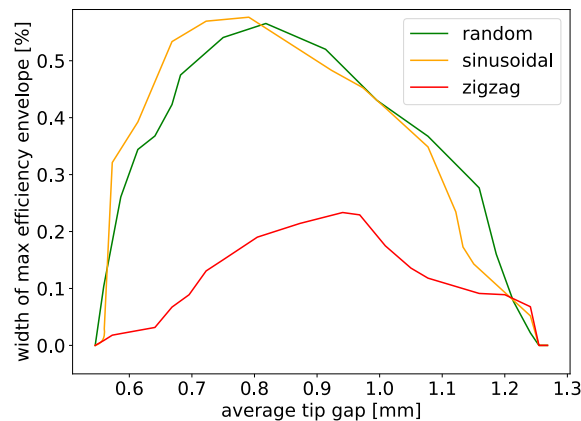


Figure 12 VERTICAL WIDTH OF MAXIMUM ISENTROPIC EFFICIENCY ENVELOPE AGAINST AVERAGE TIP GAP FOR NASA ROTOR 67

To conclude, it has been shown that the arrangement yielding best performance (sinusoidal for stagger angle and zigzag for tip gap) also yields the lowest variability. The variability largely increases if the blade arrangement is not considered or, equivalently, if the manufactured blade geometry is not measured. This shows the paramount importance of manufacturing tolerance assessment and blade arrangement on the rotor performances.

4 FUTURE WORK

To the best of author's knowledge, this is the first attempt at building a surrogate model to predict performances of a compressor with manufacturing tolerances. In future works, the model will be used to investigate the effect of tip gap variations on stall margin. Compressors with both stagger angle and tip gap variations will also be studied. Stagger angle variations can also lead to mistuning, which impacts the aeroelastic behavior of the rotor (Stapelfeldt and Vahdati, 2018). The uncertainty quantification of the flutter boundary with respect to stagger angle variations is thus another field of interest.

5 CONCLUSION

This work investigated the influence of manufacturing tolerances on a compressor's performances (total pressure ratio and isentropic efficiency). To quickly evaluate the characteristic curve of a compressor given of set of manufactured blades, a surrogate model has been developed. It relies on the physical assumption that most of the effect is on the blade itself and its neighbors, whereas the influence of further blades can be neglected. This allows to build an efficient model using few single-passage and double-passage computations, which are inexpensive. For stagger angle variations, performance can be predicted with a maximum error of 0.2% accuracy. For tip gap variations, which are more non-linear, the maximum error is 2.6%. A second step called smart average has been proposed, which halves the error at the extra cost of full-annulus computations used to optimize a set of parameters.

Given the good agreement of the surrogate model with CFD data, it has been used to investigate the effect of blade arrangement on 50,000 sets of manufactured blades. For each set, three arrangements have been studied:

- random, which is representative of not measuring blade geometry
- sinusoidal, which minimizes the variation between two adjacent blades
- zigzag, which maximize the variation between adjacent blades

The results confirmed that minimizing the variation between adjacent blades is beneficial for stagger variation, whereas it needs to be maximized for tip gap variations. A new important result is the role of arrangement on performances variability. It was observed that the best arrangement reduces the spread in performances compared to random arrangement. For maximum isentropic efficiency, the range is divided by 4 for stagger angle variations and by 2 for tip gap variations.

These results were obtained on two very different rotor designs and are thus expected to be general. They may however depend on the range and the distribution (normal, gaussian, ...) of the manufacturing tolerances. Following the methodology described in this work, one can build their own surrogate model. The performances variability can then be assessed by using the company's own data on manufacturing tolerances.

References

- Dodds, J. and Vahdati, M. (2015), 'Rotating stall observations in a high speed compressor-part 2: Numerical study', *ASME J. Turbomach.* **137**(5), 051003.
- Gopinathrao, N. P., Bagshaw, D., Mabilat, C. and Alizadeh, S. (2009), Non-deterministic cfd simulation of a transonic compressor rotor, *in* 'Turbo Expo: Power for Land, Sea, and Air', Vol. 48876, pp. 1125–1134.
- Kirk, J. (2014), 'Genetic algorithm based traveling salesman problem. Retrieved On December 12, 2018 From MATLAB Central File Exchange'.
- Kolmakova, D., Baturin, O. and Popov, G. (2014), Effect of manufacturing tolerances on the turbine blades, *in* 'ASME 2014 Gas Turbine India Conference, GTINDIA', Vol. 12, p. 30.
- Lange, A., Voigt, M., Vogeler, K., Schrapp, H., Johann, E. and Gümmer, V. (2012), 'Impact of manufacturing variability on multistage high-pressure compressor performance', *Journal of engineering for gas turbines and power* **134**(11).
- Lavainne, J. (2003), Sensitivity of a compressor repeating-stage to geometry variation, PhD thesis, Massachusetts Institute of Technology.
- Lee, K. B., Wilson, M. J. and Vahdati, M. (2018), 'Validation of a numerical model for predicting stalled flows in a low speed fan - part 1: Modification of spalart-allmaras turbulence model', *ASME J. Turbomach.* **140**(5), 051008.
- Liu, Z. Y., Wang, X. D. and Kang, S. (2014), Non-deterministic cfd simulations on the effect of uncertain tip clearance on an axial rotor performance, *in* 'Advanced Materials Research', Vol. 860, Trans Tech Publ, pp. 1499–1505.
- Loeven, A. and Bijl, H. (2010), The application of the probabilistic collocation method to a transonic axial flow compressor, *in* '51st AIAA/ASME/ASCE/AHS/ASC structures, structural dynamics, and materials conference 18th AIAA/ASME/AHS adaptive structures conference 12th', p. 2923.
- Ma, C., Gao, L., Li, R., Wu, Y. and Jiang, H. (2019), Uncertainty analysis of aerodynamic performance for tip clearance size of compressor, *in* 'Beijing Conference 2019', pp. 1–8.
- Montomoli, F., Massini, M. and Salvadori, S. (2011), 'Geometrical uncertainty in turbomachinery: Tip gap and fillet radius', *Computers & Fluids* **46**(1), 362–368.

- Sayma, A. I., Vahdati, M., Sbardella, L. and Imregun, M. (2000), 'Modeling of three-dimensional viscous compressible turbomachinery flows using unstructured hybrid grids', *AIAA J* **38**(6), 945–954.
- Stapelfeldt, S. and Vahdati, M. (2018), 'On the importance of engine-representative models for fan flutter predictions', *Journal of Turbomachinery* **140**(8).
- Strazisar, A. J., Wood, J. R., Hathaway, M. D. and Suder, K. L. (1989), Laser anemometer measurements in a transonic axial-flow fan rotor, Technical Publication NASA-TP-2879, Lewis Research Center, NASA, Cleveland, OH.
- Suriyanarayanan, V., Rendu, Q., Vahdati, M. and Salles, L. (2022), 'Effect of manufacturing tolerance in flow past a compressor blade', *Journal of Turbomachinery* **144**(4).
- Vahdati, M. and Imregun, M. (1996), 'A non-linear aeroelasticity analysis of a fan blade using unstructured dynamic meshes', *Proceedings of the IMechE, Part C - J. Mech. Eng. Sci.* **210**(6), 549–564.
- Vahdati, M., Sayma, A. I., Freeman, C. and Imregun, M. (2005), 'On the use of atmospheric boundary conditions for axial-flow compressor stall simulations', *ASME J. Turbomach.* **127**(2), 349–351.